https://rbgeomorfologia.org.br/
ISSN 2236-5664

Revista Brasileira de Geomorfologia

v. 24, nº 2 (2023)

http://dx.doi.org/10.20502/rbg.v24i2.2337

Research Article

Morphology, flow structure, and sediment transport in the Paraná and Piquiri Rivers confluence, Brazil

Morfologia, estrutura de fluxo e transporte de sedimentos na confluência dos rios Paraná e Piquiri, Brasil

Altair Bennert.[1], Ericson Hideki Haykawa[2], Isabel Terezinha Leli[3], José Cândido Stevaux[4]

[1] Western Paraná State University, Unioeste – Graduate Program in Geography, Marechal Cândido Rondon, PR, Brazil. E-mail. bennert.geo@gmail.com
ORCID: https://orcid.org/0000-0001-8230-2288

[2] Western Paraná State University, Unioeste – Graduate Program in Geography, Marechal Cândido Rondon, PR, Brazil. E-mail: ericson.hayakawa@unioeste.br
ORCID: https://orcid.org/0000-0003-1342-1659

[3] Western Paraná State University, Unioeste – Graduate Program in Geography, Marechal Cândido Rondon, PR, Brazil. E-mail. isabeltleli@gmail.com
ORCID: https://orcid.org/0000-0002-4344-3739

[4] Federal University of Mato Grosso do Sul - UFMS/CPTL – Graduate Program in Geography, Três Lagoas, MS, Brazil. E-mail. josecstevaux@gmail.com
ORCID: https://orcid.org/0000-0001-6136-2556

Received: 16/12/2022; Accepted: 06/03/2023; Published: 14/06/2023

Abstract: Confluences are places of a complex interaction of flow and sediments coming from different channels. Studies at large confluences have advanced the understanding of these environments on a larger scale. This study is carried out at the confluence formed by the Paraná and Piquiri rivers in the state of Paraná - Brazil. This study aimed to the analysis of channel morphology, flow structure, and sediment dispersion at the confluence of rivers. The methodology consists of bathymetric data, ADCP data – Acoustic Doppler Current Profiler, and calculating suspended and bed sediment transport. ADCP data was processed in VMT software and generated the following information: flow direction, sediments load (bed and suspended) and used to calculate the moment ratio (M_r), discharge ratio (Q_r), stream power (Ω), and specific stream power (ω) in both channels. The results reveal the variation of channel depth, and specific morphological areas for the confluence with a sediment accumulation zone, submerged lateral bar, and excavation area. The flow dynamics shows an increase in velocity in the Paraná River downstream of the confluence and a decrease in the flow velocity of the Piquiri River as it approaches the junction. The confluence has a flow stagnation zone, acceleration, and shear layer. The suspended sediment concentration is higher in the Piquiri River, on the other hand, the bed material of the Paraná River is predominantly composed of medium to coarse sand fractions.

Keywords: confluence, morphodynamics, channel planform, suspended sediment concentration.

Resumo: Confluências são locais de complexa interação de fluxo e sedimentos provindos de canais diferentes. Estudos em grandes confluências tem avançado na compreensão destes ambientes em escala maiores. Este estudo é realizado na confluência formada pelos rios Paraná e Piquiri no estado do Paraná-Brasil. Este estudo teve como objetivo caracterizar a morfologia, estrutura do fluxo e a dispersão de sedimentos na confluência dos rios. A metodologia consistiu em analisar dados batimétricos, ADCP - Acoustic Doppler Current Profiler e estimar os sedimentos suspensos e de fundo. Os dados do ADCP foram processados no software VMT e geraram as seguintes informações: direção e velocidade de fluxo; estimativa da

quantidade de sedimentos suspensos além de serem base para o cálculo da razão do momentum do fluxo (M_r), razão da vazão (Q_r), *potência de canal (Ω), e potência específica de canal* (ω) em ambos os canais. Os resultados apontam para a variação de profundidade dos canais, e áreas morfológicas especificas para a confluência com uma zona de acúmulo de sedimentos, barra lateral submersa e área de escavação. A dinâmica do fluxo apresenta um aumento de velocidade no rio Paraná a jusante da confluência, e diminuição da velocidade do fluxo do rio Piquiri quando se aproxima da junção. A confluência conta com zona de estagnação de fluxo, aceleração e camada de cisalhamento. A concentração de sedimentos suspenso é maior no rio Piquiri, por outro lado o material de leito do rio Paraná é composto predominantemente por frações de areia média a grossa.

Palavras-chave: confluência, morfodinâmica, forma do canal, concentração de sedimentos suspensos.

1. Introduction

River confluences are frequent features of river networks, regardless of channel magnitude, regime, and pattern (KENWORTHY; RHOADS, 1995). Changes occur in these locations, both in the hydraulic and bed geometry, as well as in the flow structure and sediment discharge (BEST, 1987, 1988; ROY, 2008; RICE et al., 2008; RHOADS et al., 2009). Confluence studies are based on the analysis of field data, laboratory, and numerical modeling. They are generally aimed at morphological identification of the bed and flow structure to characterize local hydrodynamics, as well as changes in space and time (KENWORTHY; RHOADS, 1995; PARSONS et al., 2008; RICE et al., 2008; ROY, 2008). Confluence comprises different sub-environments that are determined by, 1) confluence angle and shape, 2) interaction between the channels flow, 3) channel discharge ratio (MOSLEY, 1976; BEST, 1987), 4) sediment transport and deposition dynamics, and 5) unconformity of beds (BIRON et al., 1993; BEST; RHOADS, 2008).

The confluence zones are morphologically classified according to erosion or deposition into excavation zone, tributary bar, central bar, lateral bar, and sediment accumulation zone (MOSLEY, 1976; BEST, 1986, 1987, 1988; BIRON et al., 1993; BEST; RHOADS, 2008). These are influenced by flow conditions such as i) *the zone of stagnation/deflection* is formed by the deflection of the streams involve and is associated with an increase in pressure and depth, and with a decrease in the speed of flux and frictional stress; ii) *the zone of separation* acts reducing the effective flow section area forming a low pressure and recirculation zone with fine sediment accumulation, iii) *the zone of maximum velocity* is related to the joining of flows after the separation zone, it is commonly associated with increasing frictional stress; iv) *the zone of flow restoration* is where the gradual recovery of the flow takes place; and v) *the zone of shear layer* is formed along the boundary of stagnant areas and the flow, it is characterized by intense turbulence, frictional stress, and well-organized flow structure (MOSLEY, 1976; BEST, 1986, 1987; BIRON et al., 1996; WEBER et al., 2001; BOYER et al., 2006; SUKHODOLOV,2001; SANTOS; STEVAUX, 2017). Until the 1980s, studies focused mainly on small confluences through laboratory experiments. Pioneering studies by Mosley (1976), Best (1987, 1988), and Roy et al. (1988) identified the major flow zones, morphology, hydraulics, and sedimentology of small confluences. Since 1990, studies of large confluences are more common with bases mainly on the characterization of these environments. For example, Best and Ashworth (1997) identified the excavation zone, lateral bars, and sediment accumulation zone at the confluence of the Jamuna and Ganges rivers.

Recently, Johnson (2017), Rhoads and Johnson (2018) and Marinho et al. (2022) characterized the excavation zone, lateral bar, and flow conditions as the shear layer, secondary flow, separation, and flow acceleration at the confluence of the Wabash and Embarras rivers, Illinois-Indiana, USA, and Branco and Negro rivers, Amazon Basin, Brazil, respectively. At the confluence of the Negro and Solimões rivers, in the Amazon basin, the variables of flow velocity, mixture conductivity, turbidity, pH, and water temperature were identified by Laraque et al. (2009). Franzinelli (2011) found a 40 m deep excavation zone downstream of the confluence and the absence of upstream avalanche face morphology, which does not happen in small confluences. In this confluence, Nascimento (2016) detected an erosion zone, a submerged lateral bar, and areas with different flow behaviors responsible for the stagnation, deflation, separation, and flow recovery zones, those typical in small confluences. Siqueira and Filizola Jr. (2021) verified that the divergence between the channel bed, the confluence angle and the momentum flow ratio are the probable factors of the interference of the Negro River on the Tarumã-Açu River.

In the Upper Paraná River, Brazil, the confluence studies characterized the morphological (MORAIS et al., 2016; and LELI et al., 2022), flow behavior, and suspended sediment distribution (FRANCO, 2007; PAES, 2007; SANTOS, 2015; GRZEGORCZYK, 2016), and in the Lower Paraná River, Argentina, concerning the flow dynamics,

island influence, morphology, and the relationship between flow structure and sediment distribution (PARSONS et al., 2007; LANE et al., 2008; SZUPIANY et al., 2009). Confluence studies in the Paraná River are still relevant since the channel is formed by different and complex processes of flow and sedimentation due to its anabranching pattern. The wide variety of processes in confluences of this system represents a great laboratory for understanding the flow and transported sediments behavior, as well as the processes and morphological responses of the Piquiri-Paraná confluence. This condition deserves to be highlighted due to the need to elucidate some gaps in the confluence processes of this system, mainly in the characterization of the secondary flow, flow direction, and distribution of suspended sediment concentration. In this context, the main goal is to characterize the morphology, flow structure, and sediment dispersion for these confluence environments.

We studied the Piquiri (RPQ) and Paraná (RPR) confluence, where the Piquiri River is the tributary in the Paraná River that has an anabranching pattern formed by the Ilha Grande island. In addition, it characterizes the channel bed unconformities and the water temperature difference between the two channels.

2. Study area

The confluence of the Piquiri River is at the end of the only reach (235 km) of the Upper Paraná River without damming, between the Porto Primavera dam and Itaipu reservoir. The mouth of the Piquiri River occurs 15 km upstream of the Itaipu reservoir on the left bank of the Paraná River (54º 05′ 38″ W and 24º 01′ 38″ S). Ilha Grande island, which represents the largest island in the Upper Paraná, is almost 100 km long, with a variable width of up to 9.3 km, and is responsible for causing one of the largest anastomoses with active channels in the world. The total width of the channel in this section varies between 6 and 12.5 km, and the channel on the left bank of Ilha Grande is narrower, between 0.5 and 1.7 km than the right, which varies between 0.6 and 8 km in width. Confluence studied area covers an extension of 2.6 km in the Piquiri River, and in the Paraná River, it comprises 2.8 km upstream to 3.1 km downstream from the confluence (Fig. 1).

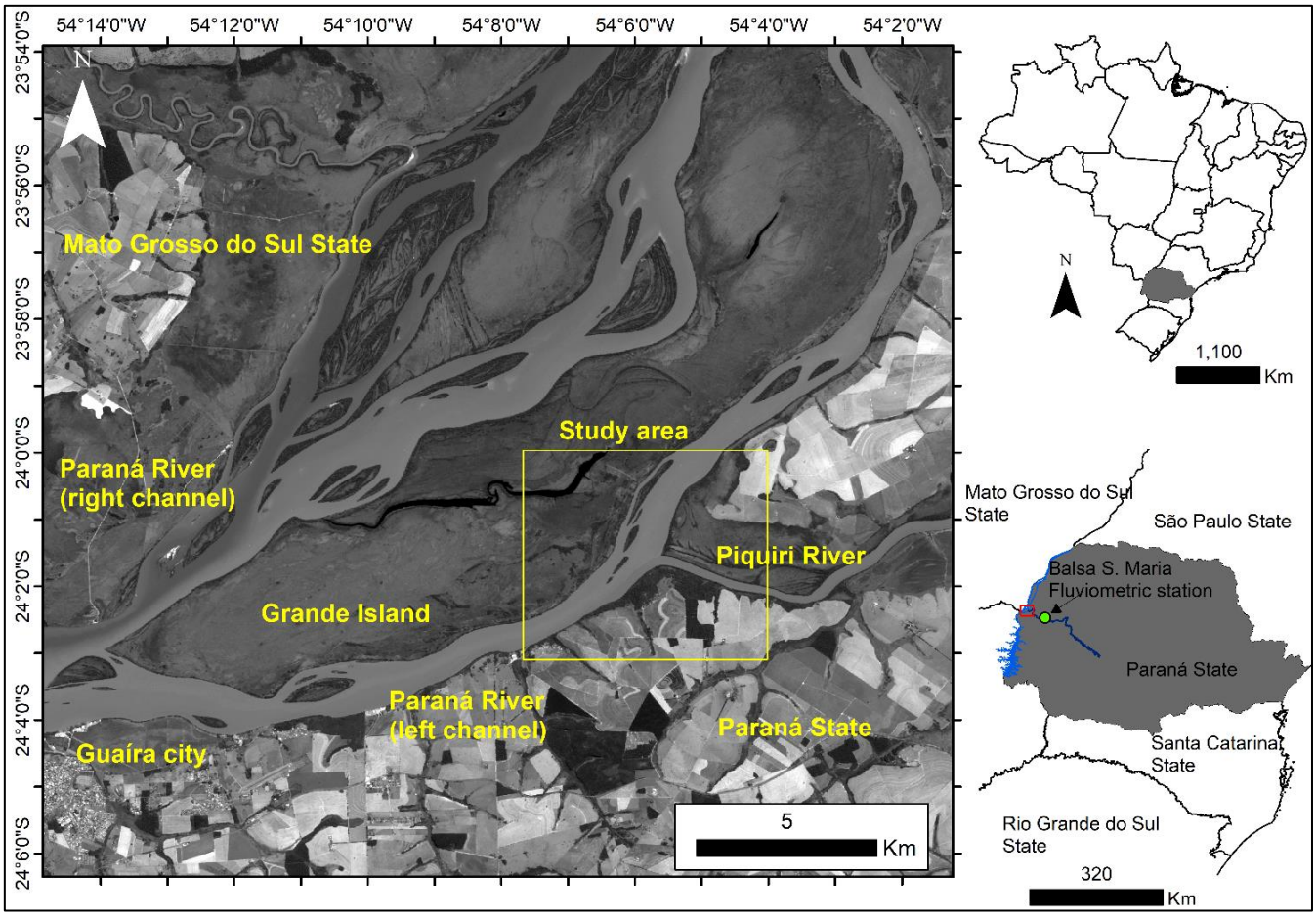

Figure 1. Paraná and Piquiri rivers, and confluence location. Source: Landsat-8/OLI image, path/row 224/77 of August 8th, 2015, Band-8 - pancromatic.

At the confluence the drainage area of the Paraná River basin is 950 km². The area is in the Umuarama Plateau, with medium dissection, elongated and plane tops, convex hillside, and valley in 'V' (SANTOS et al., 2006). The confluence zone has a floodplain formed for both channels with approximately 10,6 km². The geology of the area is formed by the basalts of the Serra Geral Fm. and sandstones of the Caiuá Fm. (MINEROPAR, 2001).

The Paraná River average flow of the Guaíra fluviometric station (1920 to 2014) is 11,130 $m^3 s^{-1}$, with extremes of 2,490 $m^3 s^{-1}$ (1944), and 39,852 $m^3 s^{-1}$ (1983). The Piquiri River average flow of the Balsa Santa Maria fluviometric station (1980 to 2016) is 532.8 $m^3 s^{-1}$, with extremes of 75.1 $m^3 s^{-1}$ (1985) and 8,406 $m^3 s^{-1}$ (2014) (Fig. 1). The suspended sediment concentration is very different between these rivers due the dams in the Upper Paraná River. Only the Porto Primavera Dam (227 km upstream) reduced the suspended sediment concentration from 25 mg L^{-1} to 0.3 mg L^{-1} (STEVAUX et al., 2009). In turn, the Piquiri River transports between 46 and 140 mg L^{-1}, dumping an average of 5,000-ton d^{-1} of suspended sediment into the Paraná River (LIMA et al., 2004).

2. Methods

Fieldwork was carried out between December 7 and 11, 2016, in the high-water level flow phase of both rivers. The bathymetric survey was carried out with a Furuno echo sounder (GP-1650F) through a mesh of zigzag sections between the banks. Flow discharge and velocity readings were obtained by 600 kHz Acoustic Doppler Current Profiler (ADCP) River Ray Teledyne RDI (Thousand Oaks, CA) (MUELLER et al., 2013; LATOSINSKI et al., 2014) in 15 cross-sections. Bed and suspended sediments were sampled at 32 points using a standard Van Veen grab sampler for the first case and a Van Dorr bottle at 20 and 50% depth for water samples. Bathymetric data (X, Y, and Z) were exported from Fugawi 4.5 software in txt extension, later accessed in ArcMap software for interpolation by the common kriging method. The RMSE obtained from the bathymetric map is 0,31. The methodological protocols of interpolation were respected, such as semivariogram analysis and mean distribution of points. ADCP data were processed in WinRiver II, then exported in ASCII file format and processed in Velocity Mapping Toolbox (VMT) software (PARSONS et al., 2013) with the base on the Matlab system to generate flow graphs (velocity, primary and secondary direction, and backscatter). The VMT software is based on the Matlab environment allowing post-processing of the analysis and display of ADCP sections (PARSONS et al., 2013; ENGEL; JACKSON, 2016). The ASCII files were converted and saved in Matlab format (*.mat) with the VMT software for the two-dimensional mapping of flow velocity and direction. Then, the section files were processed again by the VMT software to obtain the flow direction and velocity. The identification of the secondary flow in the vertical section was analyzed by the VMT software based on the Rozovskii method (1957) which identifies the secondary planes in the vertical cross-section, and the variations of the main flow without distorting the results of the secondary flow (SZUPIANY et al., 2009). The texture of the bottom sediment was obtained by sieving, and the concentration of the suspended sediment was by filtering and burning the organic matter in a muffle (ORFEO, 1995; LELI, 2010; LELI et al., 2010). The measurement of suspended sediment concentration from the ADCP backscatter signal intensity (dB) was obtained by the relation of suspended concentration from samples in different verticals (the higher the concentration the higher the backscatter values). A detailed explanation of this methods can be found in Dornelles (2009), Szupiany et al. (2009), and Latosinski et al. (2014). Backscattering data were adjusted ranging from 60 and 90 dB to facilitate comparison between the Paraná and Piquiri rivers. The bedload sediments were estimated according to Suguio (1973) and Carvalho (1994). ADCP data were also used to calculate the discharge ratio (*Qr*) Eq. 1, moment ratio (*Mr*) Eq. 2, stream power (Ω) Eq. 3, and specific stream power (ω) Eq.4 in both channels, according to the equations:

$$Qr = \frac{Qt}{Qm} \quad (1)$$

where *Qr* is the discharge ratio, *Qt* is the tributary discharge, *Qm* is the main river discharge,

$$Mr = \frac{\rho t\ Qt\ Vt}{\rho m\ Qm\ Vp} \quad (2)$$

where *Mr* is the momentum ratio, ρt is the water density of the tributary, ρm is the water density of the main river, Qt is the tributary discharge, Qm is the main river discharge, Vt is the flow velocity (m s^{-1}) of the tributary and Vp is the flow velocity (m s^{-1}) of the main river.

$$\Omega = \rho \, g \, s \, Q \quad (3)$$

where ρ is the water density (1000 kg m^{-3}), g is the gravitational constant (9.8 m s^{-2}), s is the hydraulic slope and Q is the discharge (m^3 s^{-1})

$$\omega = \Omega / w \quad (4)$$

where w is the channel width.

$Mr < 1$ indicates the dominance of the main channel flow at the confluence and >1 of the tributary (BEST, 1987; DE SERRES et al., 1999). The hydraulic slope was measured in both rivers by the Manning equation (v= 〖Rh〗 ^0,67. s^0,5/n), where v is the average flow velocity, Rh is the hydraulic radius and n is the roughness coefficient 0.025 for the Parana River (sandy bed) and 0.020 for the Piquiri River (muddy bed). We also considered the hydraulic slope calculated by Leli (2015) in the Paraná River reach by the DGPS survey. Graphs were created in Python language (matplotlib package) (HUNTER, 2007) and plotly.py package and maps in ArcMap 10.5.1 licensed in the Cartography and Geoprocessing Laboratory. We estimated bad load transport according to Suguiu (1973) and Carvalho (1994). The samples of bed load were taken to the oven for drying. 50g was weighed for each sample. The material was stirred in sieves with different mesh openings, under agitation for 20 minutes to determine the granulometry. The sediments were weighed separately according to their granulometry.

3. Results

3.1 Confluence framework and morphology

In the reach upstream the confluence, the Paraná River present a typical anabranching pattern with several islands and sandy bars and its channel does not present a defined talweg (Fig. 2). This is a typical morphology of anabranching sandy rivers (STEVAUX; LATRUBESSE, 2017), where the depth rarely exceeds 4 m at the average water level (a.w.l.), and when occurs, it is in the form of isolated pools of 5 to 6 m (a.w.l). The presence of elongated islands and sandy bars on the right bank (Fig. 2A) suggests that the channel is under a sedimentation trend from this bank to the confluence area.

After the confluence, the Paraná channel reduces its width by 35%, going from 1011 to 670 m, developing a well-defined talweg near the confluence, and dissipation downstream forming a sequence of 9 to 10 m deep pools related to the mean water level (a.w.l.) (Fig. 2B). The Piquiri River presents a well-defined and continuous talweg displaced to the channel left bank with depth between 8 and 10 m (a.w.l.) (Fig. 2C). The talweg advances the trunk river developing a well-defined curve that goes around a lateral bar with 2.5 m (a.w.l.) submerged and 900 m length after the confluence. The upstream portion of the confluence presents a deposition zone with a depth of 1 m (a.w.l.) (Fig. 2A).

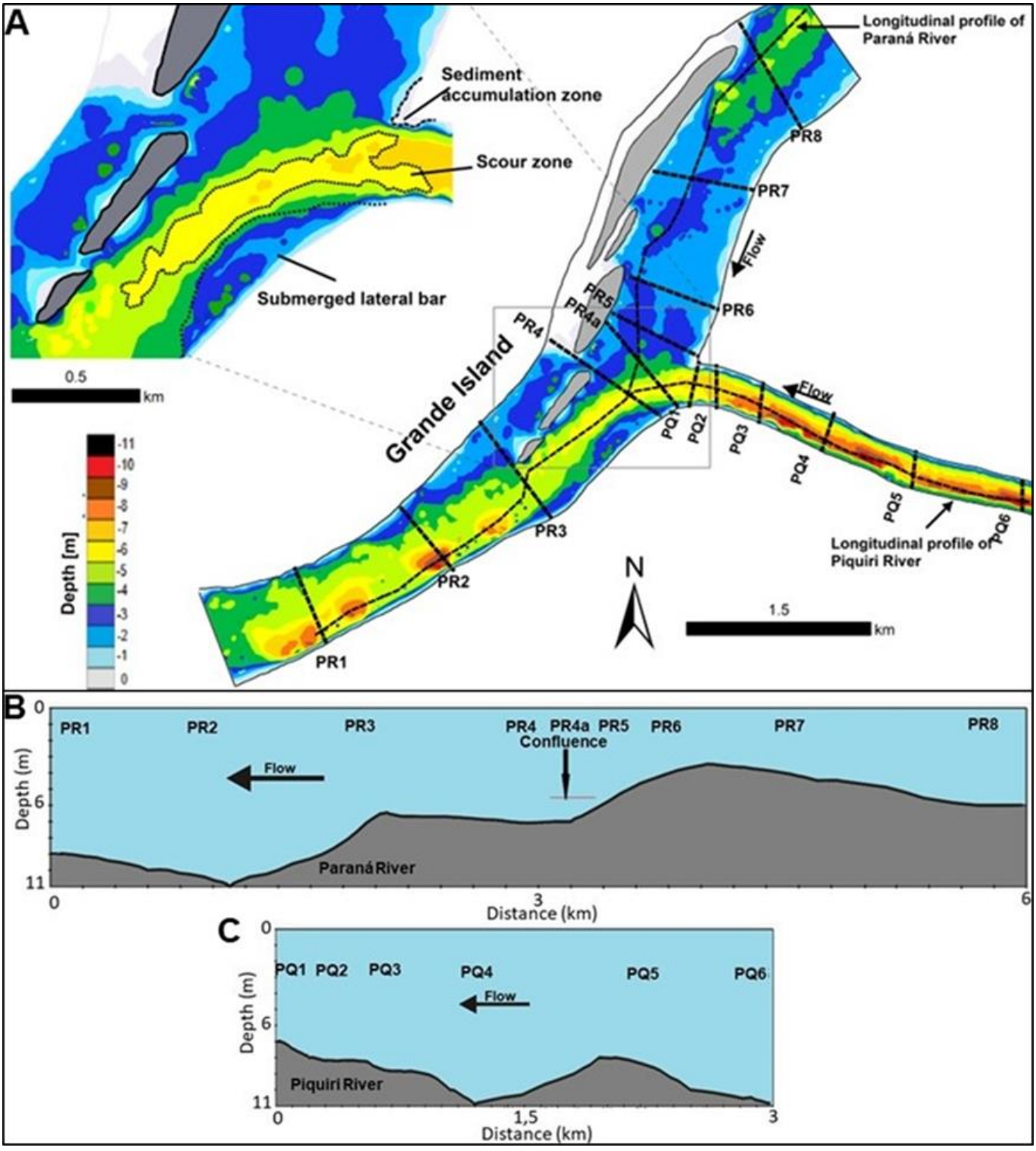

Figure 2. A) Bathymetric map of the Paraná-Piquiri confluence. In detail, one can differentiate the morphological zones: sedimentation upstream of the confluence, submerged lateral bar on the left bank of the Paraná River (depth: 2.5 m, length: 900 m), and excavation downstream of the confluence; B-C) Longitudinal bathymetric profile of the Paraná and Piquiri channels.

3.2 Hydrology and hydraulics

The contribution of the Piquiri River flow to Paraná is relatively low (Qr = 0.005), however, the confluence condition occurs in the secondary channel of the Paraná River, increases this relationship by 6 times (Qr = 0.30), (Tab. 1). This condition confers great importance to the changes that the confluence introduces at the local since the flow of Paraná upstream from the confluence is 2,414 $m^3 s^{-1}$ (PR8), and downstream, after receiving 727 $m^3 s^{-1}$

of the Rio Piquiri exceeds 3,000 $m^3 s^{-1}$ (PR4). Flow velocity upstream is 0.7 m s^{-1} (PR8), being reduced a little at the confluence, probably due to the hydraulic "jetty" effect (A hydraulic jetty occurs when the tributary flow keeps its direction entering in the trunk river) of the Piquiri flow (PR4). Velocity increases to 0.8 m s^{-1} downstream (PR1). The same occurs with the stream power and specific stream power whose values gradually decrease from 1490 W m^{-1} and 1.5 W m^{-2} in upstream reach (PR8) to 1088 W m^{-1} and 1.3 W m^{-2} at the confluence local (PR5) due to flow velocity reduction, and after the confluence, became 1515 W m^{-1} and 2.2 W m^{-2} (PR1).

Table 1. Hydraulic parameters of Paraná and Piquiri rivers.

Paraná River donwstream confluence sections							
Section	Q ($m^3 s^{-1}$)	v (m s^{-1})	w (m)	dm (m)	s	Ω (W m^{-1})	ω ($W m^{-2}$)
PR1	3,090.90	0.816	674.5	6.2	0.00005	1,514.50	2.2
PR2	3,075.50	0.778	681.2	6.3		1,506.90	2.2
PR3	3,076.20	0.767	962.1	4.2		1,507.30	1.5
PR4	3,068.70	0.8	1,092.70	4		1,503.60	1.3
PR4a	2,494.00	0.711	893.8	4		1,222.00	1.3
Paraná River upstream confluence sections							
PR5	1,850.30	0.66	812.4	3.5	0.00006	1,087.90	1.3
PR5	1,854.00	0.888	763.4	3.1		1,090.10	1.4
PR7	2,157.60	0.822	900.9	3.2		1,268.60	1.4
PR8	2,414.40	0.709	1,011.80	3.7		1,490.60	1.5
Piquiri River sections							
PQ1	662.70	0.398	299.7	5.9	0.000013	84.42	0.28
PQ2	706.10	0.402	267.4	6.3		89.95	0.33
PQ3	702.10	0.394	253.9	7.5		89.44	0.35
PQ4	710.00	0.384	233.2	7.9		90.45	0.38
PQ5	723.20	0.427	242.6	7.1		92.13	0.37
PQ6	727.10	0.445	206.4	8.3		92.63	0.44

The Piquiri River also has reduced its discharge downstream (PQ6 to PQ1) due to the Paraná channel damming effect, where the flow increases from 727 to 663 $m^3 s^{-1}$, the velocity drops from 0.4 to 0.3 m s^{-1}, and the same trend to Ω and ω follow, between 92.63 W m^{-1} and 0.44 W m^{-2} (PQ6) to 84.42 W m^{-1} and 0.28 W m^{-2} (PQ1) (Fig. 3 and Tab. 1).

The discharge and momentum ratios are Qr = 0.26 and Mr = 0.14 to the PQ1 and PR4A sections, and Qr = 0.38 and Mr = 0.22 to the PR5 and PQ2 sections, indicating the predominance of the Paraná River flow over the Piquiri River at the confluence. The flow stagnation zone located on the right bank of the confluence is not well defined since it develops in a reach of flow dammed by the Paraná River. This condition changes according to the flow regime of the two systems. The occurrence of a deposition zone at the local confirms the permanence of the stagnation zone in the system (Figs. 3A and 2A). This is due to the flow of the Paraná River upstream of the confluence has a strong tendency toward the confluence bank, with the highest velocities close to the islands on the right bank (Fig. 3B).

In the confluence downstream, the Piquiri River water keeps on the left bank in the Paraná channel, occupying a large part of the talweg with a direction parallel to the bank, contrasting the Paraná flow direction, as well as the shear layer (Fig. 3B). We point out that although the Piquiri flow is dammed in the end reach when it enters the Paraná its velocity is doubled, obtaining conditions to former the helical flow, with evident flow separation maintenance along the left bank of the Paraná (Fig. 3C). The Piquiri water temperature has 26 °C, two degrees less than the Paraná, keep similar values when it enters the Paraná River until more than 1000 m downstream of the confluence (Fig. 4B).

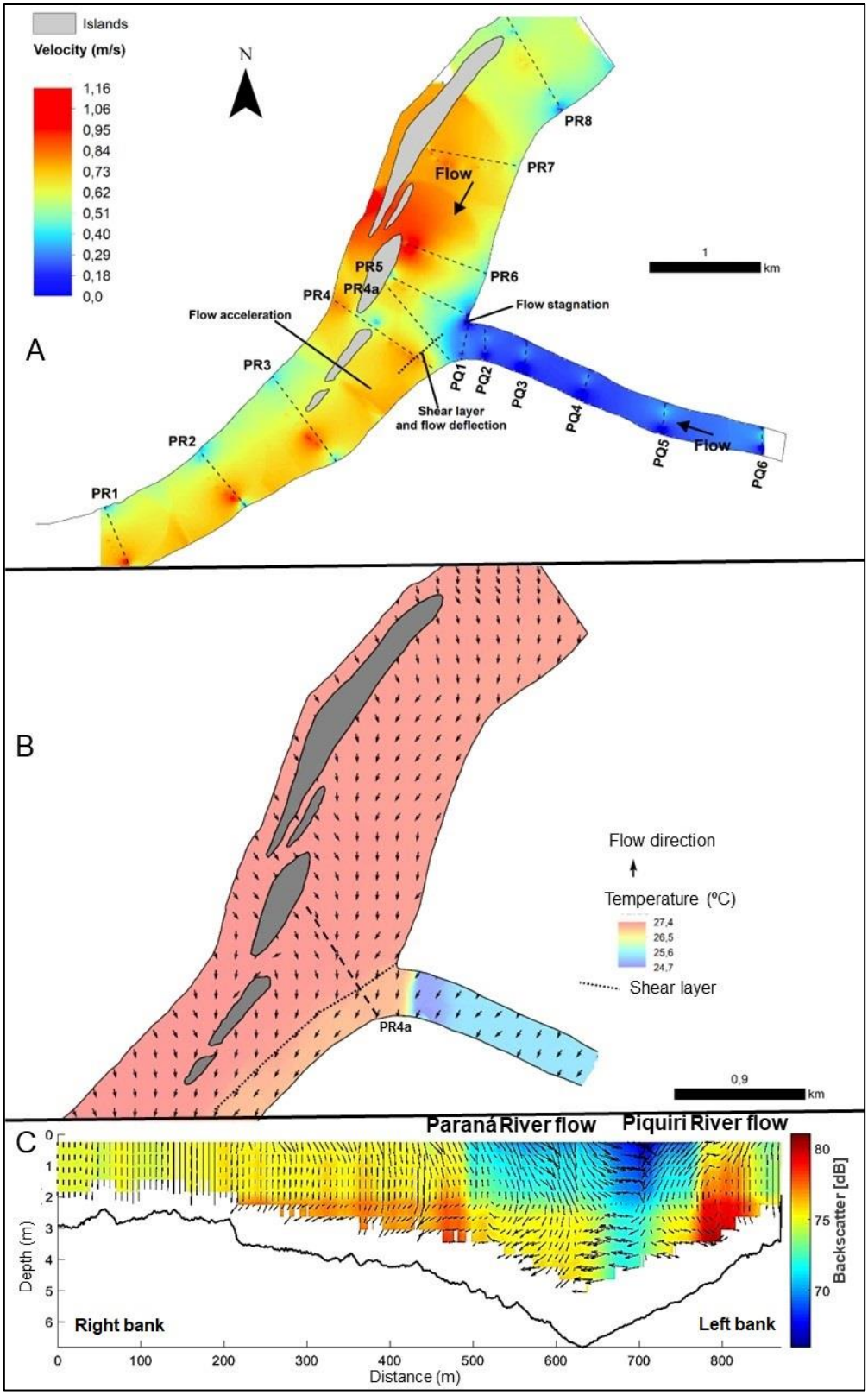

Figure 3. A) Confluence zones and flow velocity. Note the Paraná River zone of high-velocity change from the right to the left bank after the confluence, showing the Piquiri influence and the talweg development; B) Flow direction and temperature. Note the tends of the Paraná flow towards the left bank in the upstream and downstream confluence. The Piquiri flow and water temperature remain distinct in the Paraná one of confluence downstream; C) Cross-section PR4a with the secondary flow and backscatter intensity: most of the water flows downstream in the left bank by 400 m with the secondary flow cells of helicoidal flow, and the backscatter values increased according to the higher concentration of suspended sediment from the Piquiri River.

3.3 Suspended sediment

Among the total of 74 samples of sediment suspended in the two channels, 30 samples from the Paraná River show an average of 20.9 mg L^{-1} ranging from 13.8 mg L^{-1} to 42 mg L^{-1}, while in 3 samples from the river Piquiri the average is 26.8 mg L^{-1}, and ranges from 18.4 mg L^{-1} to 46.6 mg L^{-1} (Fig. 4).

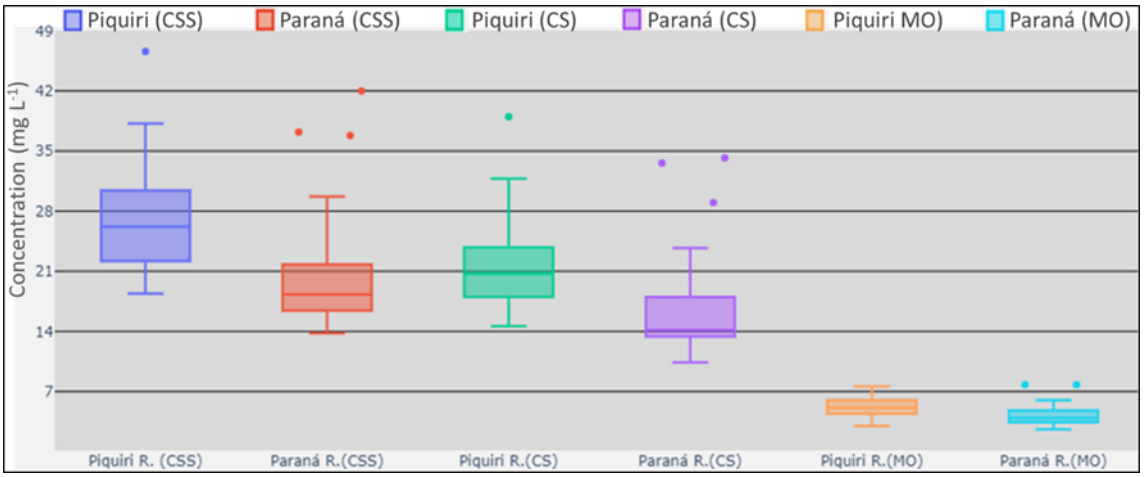

Figure 4. Boxplot for suspended sediment concentration total (Css), mineral (Cs), and organic material (MO). Colored points are outliers values of suspended sediment sample.

According to the suspended sediment data at the Guaíra station, Paraná, the Paraná River transports 10,233 ton.day^{-1} for an average flow of 10,603 m^3 s^{-1}. Leli (2015) found that the left channel of the Paraná River (confluence channel) holds 35% of the flow of the right channel, which made it possible to quantify the transport of suspended sediment from the left channel at 3581 ton day^{-1}. The spatial distribution of the suspended load obtained through the correlation between the ADCP Backscatter values in decibels (dB) and the suspended sediment concentration (Css) from the samples collected show good correlations of R^2 = 0.7104 for the Paraná River and R^2 = 0.8243 for the Piquiri (Fig. 5).

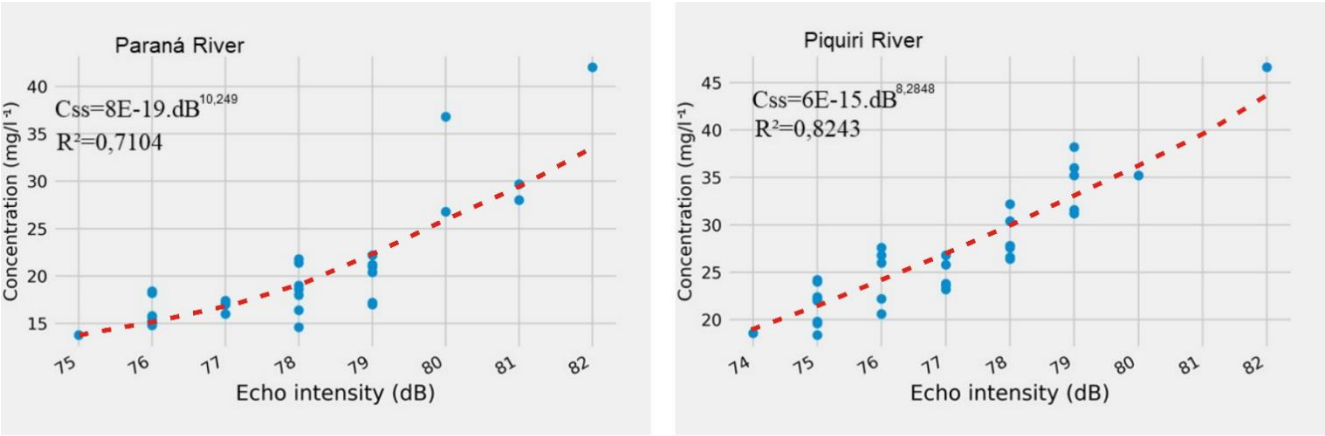

Figure 5. Rating curves for Css and dB de backscatter.

The rating curves were performed for both rivers due to the difference between the concentration of each system, as suggested by Weibel et al. (2022) for the Bermejo, Paraguay, and Paraná rivers.

The longitudinal distribution of Css does not vary significantly upstream and downstream of the confluence along the Paraná River, being generally between 20 and 25 mg L^{-1} for most stretches (Fig. 8). The stretches upstream

of the confluence present a more homogeneous distribution of Css in practically the entire cross-section. Two zones of greater concentration occur downstream of the confluence. One of them is due to the formation of helical flow cells close to the talweg, and the other is probably due to bank erosion, as it follows the Grande Island shoreline (Figs. 8 and 4).

The sediments concentration of the Piquiri River is higher than in the Paraná River (Fig. 6), and presents a homogeneous distribution along the stretch, except in the proximity of the confluence, probably due to the reduction in the velocity and damming of the flow that the Paraná imposes on the Piquiri.

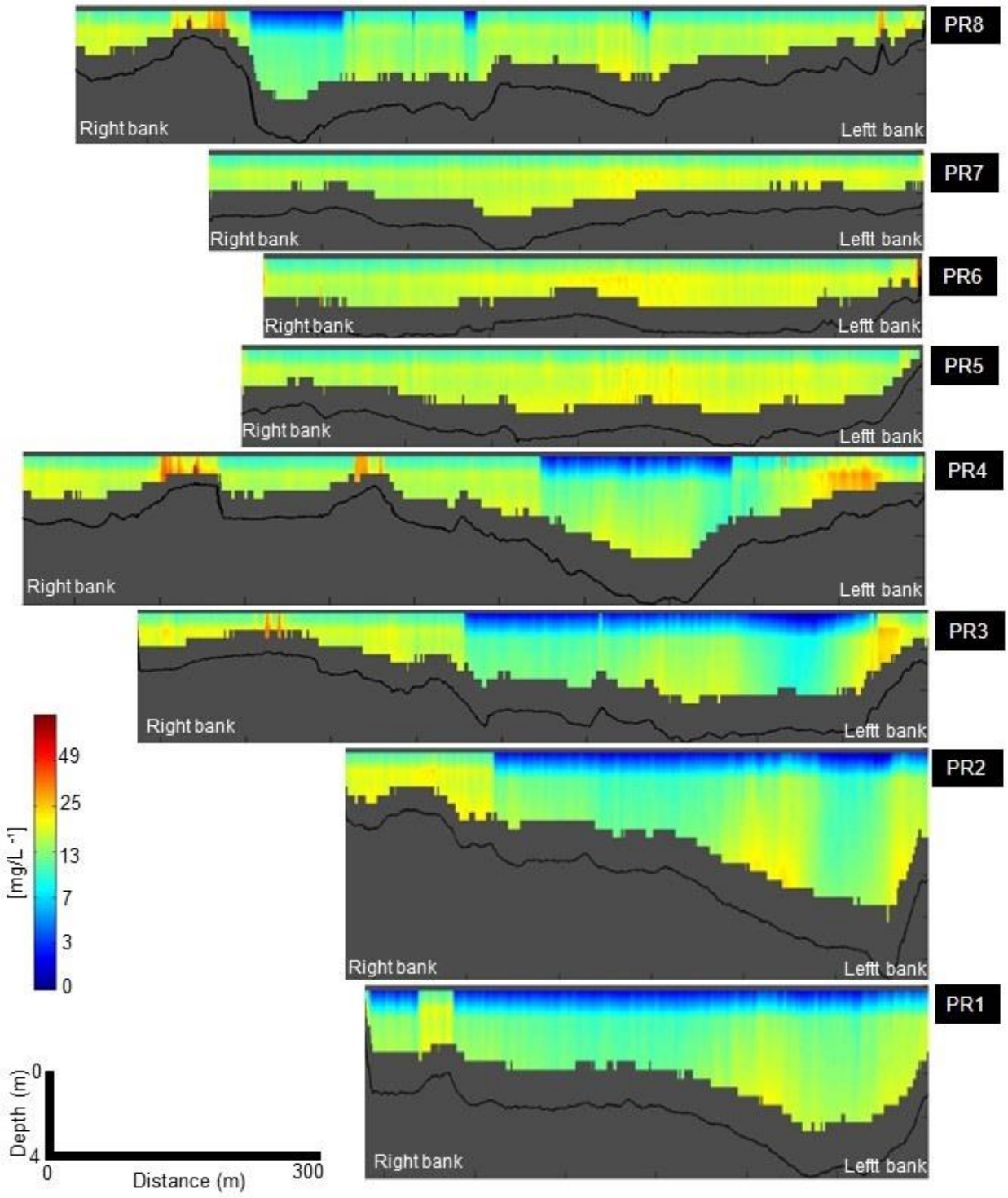

Figure 6. Paraná River cross-sections with suspended sediment concentration (Flow direction from PR8 to PR1). The abrupt variation of Css close to the water surface at the PR4, PR3 and PR2 (Blue color) is caused by inconsistence in reading of the ADCP, probably by flow perturbation.

The highest concentrations occur above 80% of the depth, with a significant reduction near the mouth, where the mixture of water from the two systems causes the dilution of the Piquiri River Css, compared to the upstream section (Fig.7).

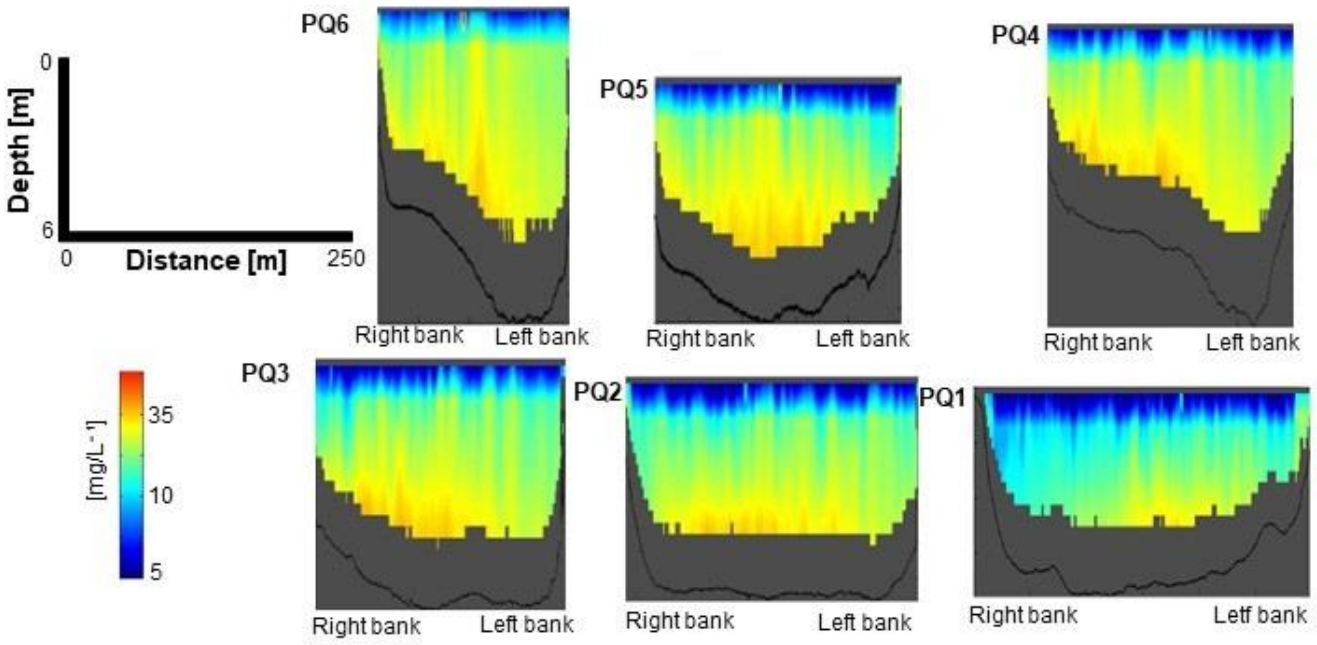

Figure 7. Piquiri River cross-sections with the suspended sediment concentration (Flow direction is from PQ6 to PQ1).

3.4 Bedload

The bed material is slightly different for both rivers. While the Paraná River presents a composition of fine to coarse sand, and localized occurrence of pebbles (Fig. 8), in the Piquiri River the finer fractions predominate, medium to fine sand in the central portions, and mud near the banks, and scattered occurrence of pebbles (Fig. 9).

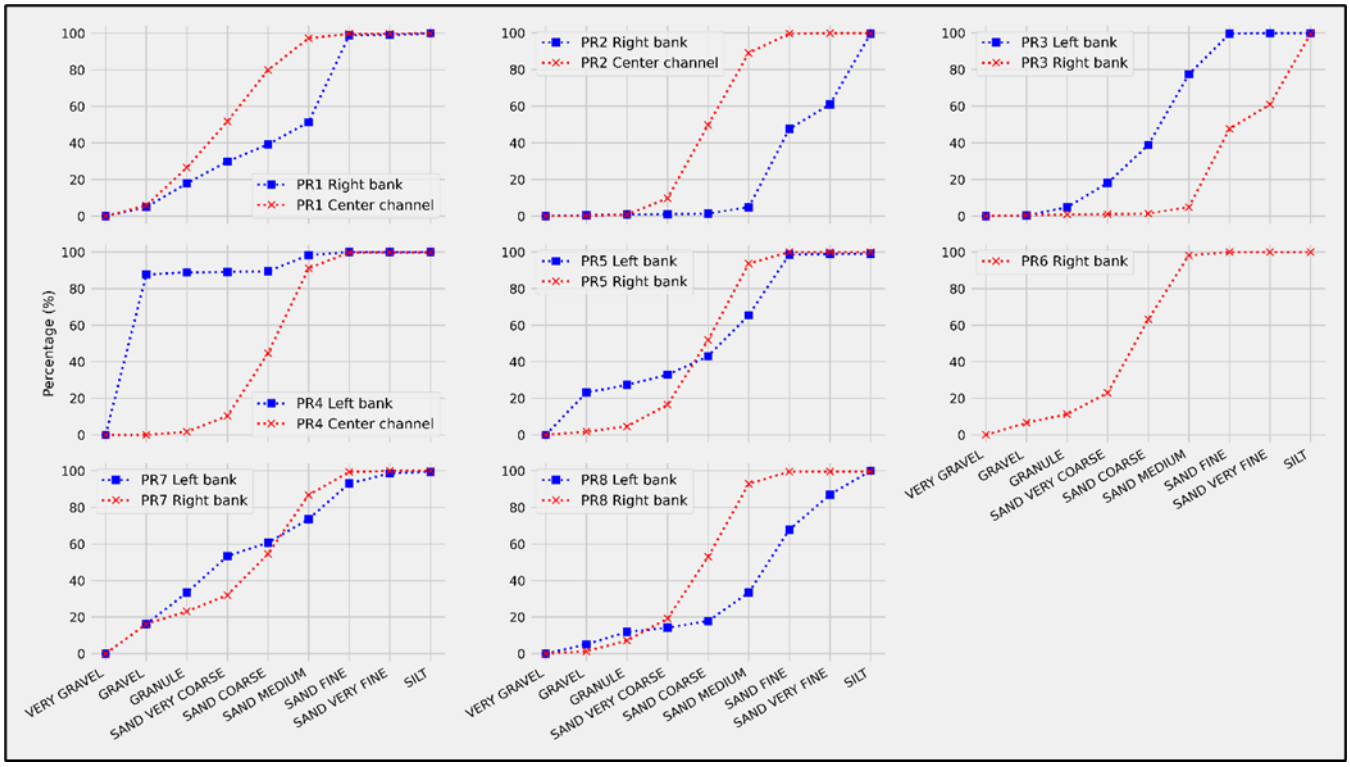

Figure 8. Percentage accumulative curve for bed material of the Paraná River.

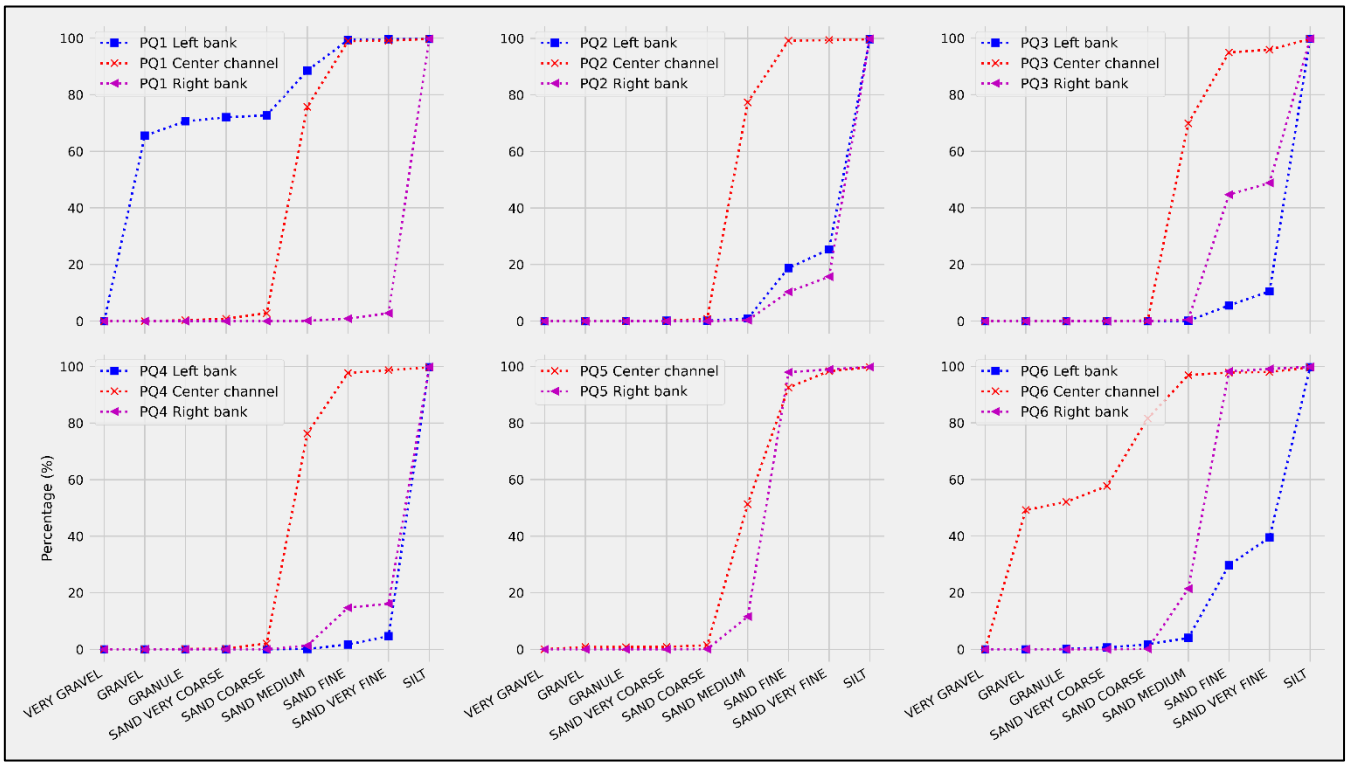

Figure 9. Percentage accumulative curve for bed material of the Piquiri River.

4. Discussion

4.1 Discussion: How does Piquiri River confluence zone differ from the other left-bank tributaries in the Upper Paraná River?

The Piquiri together with the Ivaí and Paranapanema rivers are the main left-hand tributaries of the Paraná River in the reach between the Itaipu and Porto Primavera reservoirs. The Ivaí and Parapanema rivers confluence that occurs in the Paraná nodal section, the Piquiri River confluence is different by occurring in a section of a single channel of the Paraná River. In turn, the confluence of the Piquiri River occurs in a secondary channel of the Paraná River, resulting in a *Qr* about six times higher than that of the other two tributaries. The Piquiri confluence also differs in terms of the geological substrate. In the case of the Paranapanema and Ivaí rivers, the confluence reach is alluvial, occupying a wide floodplain, while the Piquiri River flows over a rocky substrate along the contact between the sandstones of the Caiuá Formation (Late Cretaceous) and basalts from the Serra Geral Formation (Cretaceous). The condition of the Piquiri being under strong structural control produces an orthogonal confluence, different from the other tributaries whose confluence angles are 45°.

Acute angle confluences do not generate an expressive hydraulic jetty and are less susceptible to the backwater (SANTOS et al., 2022). It is the case of the Paranapanema (BARROS, 2006) and Ivaí (BIAZIN, 2005; FRANCO, 2007) rivers. In these cases, the high velocity flow zone appears just downstream the confluence in conformity with the literature's model (BEST 1987). The study confluence is orthogonal and generates a hydraulic jetty effect and a small backwater zone on the Paraná River flow. It is possible to notice the drift of the flow lines of the Paraná River to the right bank and a low velocity zone just in from of the confluence (Fig. 3A).

In the case of the two upstream mentioned tributaries the acute angle, associated with the wide nodal section of the confluence site, allowed the development of large confluence islands and long confluence channel, and consequently the formation of a *tributary mixed floodplain* (LELI; STEVAUX, 2022). The situation is different at the Piquiri River confluence, where the relatively narrow channel of the trunk river and the generation of the hydraulic jetty prevent the formation of confluence islands, as in the case of upstream tributaries.

The morphology of the Piquiri-Paraná confluence presents some characteristics that fit the model proposed by Mosley (1976), Best (1986, 1987, 1988), and Bristow et al. (1993). The stagnation zone is not expressive (Fig. 3), but it develops an accumulation zone of fine sediment that reduces the channel depth (Fig. 3). The separation zone, increased by the hydraulic jetty effect, constructs an expressive lateral bar after the confluence (Fig. 2A). Lateral bars also occur in the Ivaí and Paranapanema rivers (FRANCO, 2007; PAES, 2007), however, both are in narrow confluence of straight channels by the imposition of helical flow. In the studied case, helical flow occurs in two cells separated by the contact between the Paraná flow and the extension of the Piquiri flow after the confluence (Fig.3C). Szupiany et al. (2012) identified secondary movements and helical cells in the deepest places and the shear zone. Szupiany et al. (2009) observed that helical cells occupy a small channel area (<20%).

The bed discordance of small confluences would be another condition for secondary flow generation (BEST; ROY, 1991; BIRON et al., 1996). This is the study case, in which the bed unconformity at the confluence generates a water pressure gradient favoring secondary flow generation. The difference of 2ºC in water temperature between the Piquiri and Paraná at the confluence is caused by the climate conditions at their basins. The warmer climate of the Paraná River and the large number of dams increase the water temperature (AGOSTINHO et al., 2004). The Piquiri River runs through a region with a milder climate, with small rapids in the upper course and headwaters between 800 and 1000 m a.s.l. Besides it, the Paraná runs for 3900 km against only 600 km of the Piquiri, in this case the trunk the long path covered by the waters provides a greater mixing of the colder headwater waters with the downstream warm ones.

The development of secondary flow and the generation of helical cells at the mixing flow interface at the Paraná/Piquiri rivers confluence segregate the sediment concentration. This leads to the lowest concentration at the contact between the helical cells and favors the major sediment concentration on the left bank downstream of the mouth (Fig. 3), according to the model proposed by Best (1988).

5. Conclusion

The Piquiri and Paraná rivers confluence differ from others of the same system in many aspects: a) this confluence occurs in a secondary channel of the anabranching section of the trunk river, while the others occur in nodal sections; b) the orthogonal confluence of the Piquiri provides a hydro-sedimentary dynamics very different from the sharp-angled confluence of the other tributaries; c) the studied confluence develops in major in a rocky channel, therefore with great litho-structurally control, differing from the other alluvial channel confluences.

This confluence is formed by a zone of sediment accumulation in the upstream corner of the confluence and a (submerged) lateral bar downstream of the left bank and does not characterize all morphologies of minor

confluences. The models derived from backscatter and suspended sediments are different due to the difference between the suspended sediment concentration between the Paraná and Piquiri rivers.

Future work should measure the flow, velocity, and direction of flow mainly between islands close to the confluence. This will make it possible to better understand the role of islands in the structure and dynamics of the river flow. Bathymetric data in a more detailed scale will highlight the features of the study area; a more dense suspended sediment sampling will allow for improving the model between the backscatter and suspended sediments. Bathymetric data in the detailed scale will highlight the features of the study area and the greater number of suspended sediments will allow for improving the model between the backscatter and suspended sediment concentration. Detailed bottom sediment data, mainly in the confluence environment, will make it possible to understand their distribution at the mixing interface and their respective deposition areas.

Author's contributions: A. Bennert: Writing – review & editing, Writing – original draft, Visualization, Validation, Supervision, Project administration, Methodology, Investigation, Formal analysis, Data curation, Conceptualization. E.H. Hayakawa: Writing – review & editing, Methodology, Investigation, Data curation, Conceptualization, resources, project administration, funding acquisition. I.T. Leli: Writing – review & editing, Visualization, Validation, Supervision, Project administration, Methodology, Investigation, Formal analysis. Data curation, Conceptualization. J. C. Stevaux: Writing – review & editing, Supervision, Resources, Project administration, Methodology, Investigation, Funding acquisition, Formal analysis, Conceptualization.

Support: We thanks to the National Council of Science and Technology (CNPq/Brazil) for the financial support awarded to E. H. Hayakawa (grant #472012/2014-2 and 313757/2021-6), and José C. Stevaux (grant #304863/2015-7 and 308957/2020), and, "This study was financed in part by the Coordenação de Aperfeiçoamento de Pessoal de Nível Superior – Brasil (CAPES) – Finance Code 001".

Acknowledgment: To Mr. Ademar da Silva for supporting field activities (loaning the ship and acting as the boat's pilot), to Dr. Leandro Luz for field support, Dr. Vanessa Cristina dos Santos for the theoretical contributions, to Dr. Mário Luís Assine – Unesp/Rio Claro – SP for the ADCP loan, the Western Paraná State University for the infrastructure; to Dr. Tony Vinícius Moreira Sampaio – UFPR/Curitiba - PR for his contributions in geostatistics, to Dr. Vanderley Grzegorczyk for his suggestions, to Dr. Ótávio Cristiano Montanher for his contributions in statistics and to the reviewers.

Declaration of competing interest

The authors declare not having any conflict of interest or personal relationships that could have appeared to influence the work in this paper.

References

1. BARROS, C. S. **Dinâmica sedimentar e hidrológica na confluência do rio Ivaí com o rio Paraná, município de Icaraíma-PR**. Dissertação (Mestrado em Geografia) – Programa de Pós-graduação em Geografia, Universidade Estadual de Maringá, Maringá. 2006. 53p.
2. BEST, J.L. The morphology of river channel confluence. **Progress in Physical Geography**. v. 10, n. 2, p. 157-174, 1986.
3. BEST, J. L. Flow dynamics at river channel confluences: Implications for sediment transport and bed morphology. In: ETHERIDGE, F.G.; FLORES, R.M.; HARVEY, M.D. **Recent Developments in Fluvial Sedimentology**. SEPM: Tulsa, n. 39, 1987, p. 27-35.
4. BEST, J. L. Sediment transport and bed morphology at river channel confluences. **Sedimentology**, v. 35, p. 481-498, 1988.
5. BEST, J. L.; Roy, A.G. Mixing-layer distortion at the confluence of channels of different depth. **Nature**, v. 350, p. 411-413, 1991.
6. BEST, J. L.; ASHWORTH, P. J. Scour in large braided rivers and the recognition of sequence stratigraphic boundaries. **Nature**, v. 387, p. 275-277, 1997.
7. BEST, J. L.; RHOADS, B. L. Sediment transport, bed morphology and the sedimentology of river channel confluences. In: RICE, S.; ROY, A.; RHOADS, B. **River confluences, tributaries and the fluvial network**. John Wiley & Sons Ltd, 2008. Cap. 4, 45-72.

8. BIAZIN, P. C. **Caracterização sedimentar e hidrológica do rio Ivaí em sua Foz com o rio Paraná, Icaraima-Pr.** Dissertação (Mestrado em Geografia) – Programa de Pós-graduação em Geografia, Universidade Estadual de Maringá, Maringá. 2005. 74p.
9. BIRON, P.; ROY, A. G.; BEST, J. L.; BOYER, C. J. Bed morphology and sedimentology at the confluence of unequal depth channels. Geomorphology, v. 8, 115-129, 1993.
10. BIRON, P.; BEST, J. L. ROY, A. G. Effects of bed discordance on flow dynamics at open channel confluences. **Journal of Hydraulic Engineering**, v. 122, p. 676-682, 1996.
11. BOYER, C.; ROY, A. G.; BEST, J. L. Dynamics of river channel confluence with discordant beds: flow turbulence, bed load sedimento transport and bed morphology. **Journal of Geophysical Research, v. 111, 2006.**
12. BRISTOW, C. S.; BEST, J. L, ROY, A. G. Morphology and faceis models of channel confluences. **SPEC. Publs Int. Ass. Sediment,** v. 17, p. 91-100, 1993.
13. CARVALHO, N. O. **Hidrossedimentologia prática.** Rio de Janeiro: CPRM, 1994.
14. DE SERRES, B.; ROY, A. G.; BIRON, P. M.; BEST, J. L. Three-dimensional structure of flow at a confluence of river channels with discordant beds. **Geomorphology**, v. 26, p. 313-335, 1999.
15. DORNELLES, A. M. **Utilização de um perfilador acústico de correntes por efeito Doppler (ADCP) para a estimativa da concentração de sedimentos em suspensão (CSS).** Dissertação (Mestrado em Engenharia) – Programa de Pós-graduação em Recursos Hídricos e Saneamento Ambiental, Universidade Federal do Rio Grande do Sul (UFRGS), Porto Alegre, 2009. 126p.
16. ENGEL, F. L.; JACKSON, P. R. The Velocity Mapping Toolbox. User guide for version 4.08. USGS Science for a changing world, 2016.
17. ESRI Inc. ArcMap (versão 10.5.1). Redlands, Estados Unidos, 2016.
18. FRANCO, A. L. A. **Análise da dinâmica e estrutura de fluxo e da morfologia da confluência dos rios Ivaí e Paraná, PR/MS**. Dissertação (Mestrado em Análise Geoambiental) – Programa de Pós-graduação em Análise Geoambiental, Universidade de Guarulhos, Guarulhos, 2007. 82 p.
19. FRANZINELLI, E. Características morfológicas da confluência dos rios Negro e Solimões (Amazonas, Brasil). **Revista Brasileira de Geociências**, v. 41, n. 4, 587-596, 2011.
20. GRZEGORCZYK, V. **Geomorfologia das confluências do alto curso do Rio Paraná, um estudo dos rios: Ivaí-PR, Piquiri-PR e Ivinhema-MS.** Tese (Doutorado em Geografia) – Programa de Pós-graduação em Geografia, Universidade Estadual de Maringá, Maringá. 2016. 146p.
21. HUNTER, J. D. Matplotlib: A 2D Graphics Environment". **Computing in Science & Engineering**, v. 9, n. 3, p. 90-95, 2007.
22. JOHNSON, K. K. **Flow structure of an asymmetric large river confluence**. Dissertação (Mestrado em Geografia) – Programa de Pós-graduação em Geografia, University of Illinois at Urbana-Champaign, Illinois. 2017. 81p.
23. KENWORTHY, S. T.; RHOADS, B. L. Hydrologic control of spatial patterns of suspended sediment concentration at a stream confluence. **Journal of Hydrology**, v. 168, 251-263, 1995.
24. LANE, S. N.; PARSONS, D. R.; BEST, J. L.; ORFEO, O.; KOSTASCHUK, R.; HARDY, R. J. Causes of rapid mixing at a junction of two large rivers: Rio Paraná and Rio Paraguay. **Argentina, J. Geophys. Res**., v. 113, p. 1-16; 2008. DOI:10.1029/2006JF000745
25. LARAQUE, A.; GUYOT, J. L.; FILIZOLA, N. Mixing processes in the Amazon River at the confluences of the Negro and Solimões Rivers, Encontro das Águas, Manaus, Brazil. **Hydrological Processes**, p. 3131-3140, 2009.
26. LATOSINSKI, F. G; SZUPIANY, R. N; GARCIA, C. M; GUERRERO, M; AMSLER, M. L. Estimation of concentration and load of suspended bed sediment in large river by means of acoustic doppler technology. **Journal of Hydraulic Engineering**, 2014.
27. LELI, I. T. **Variação espacial e temporal da carga suspensa do Rio Ivaí.** Dissertação (Mestrado em Geografia) – Programa de Pós-graduação em Geografia, Universidade Estadual de Maringá, Maringá. 2010. 66 p.
28. LELI, I. T.; STEVAUX, J. C.; NOBREGA, M. T. Produção e transporte da carga suspensa fluvial: teoria e método para rios de médio porte. **Boletim de Geografia**, v. 28, p. 43-58, 2010.
29. LELI, I. T. **Gênese, evolução e geomorfologia das ilhas e planícies de inundação do Alto rio Paraná, Brasil.** Tese (Doutorado em Geociências e Meio Ambiente) – Programa de Pós-graduação em Geociências, Universidade Estadual Paulista Júlio de Mesquita Filho, Rio Claro. 2015. 123 p.

30. LELI, I. T; STEVAUX, J. C. The polygenetic floodplain of the Paraná River. **Journal of South American Earth Science,** v. 119, 2022. DOI: 10.1016/j.jsames.2022.103985
31. LELI, I.T.; STEVAUX, J.C.; BENNERT, A.; SANTOS, V.C.; LUZ, L.D. Morphological resilience at the confluence of a very low discharge creek and a large river (upper Paraná, Brazil). Journal of South American Earth Science 123, 104222, DOI: 10.1016/j.jsames.2023.104222.
32. LIMA, J. E. F. W.; LOPES, W. T. A.; SILVA, E. M.; VIEIRA, M. R. **Diagnóstico hidrossedimentológico da Bacia do Rio Piquiri.** Boletim de Pesquisa e Desenvolvimento. Planaltina, DF: Embrapa Cerrados, 2004.
33. MARINHO, R.R.; FURTADO, A.R.; SANTOS, V.C.; NASCIMENTO, A.Z.A.; FILIZOLA JUNIOR, N.P. Riverbed morphology and hydrodynamics in the confluence of complex mega rivers- A study in the Branco and Negro rivers, Amazon basin. Journal of South American Earth Scences, 118, 103969, DOI: 10.1016/j.jsames.2022.103969.
34. MINEROPAR – MINERAIS DO PARANÁ S.A. **Atlas comentado da geologia e dos recursos minerais do estado do Paraná. Curitiba, 2001.**
35. MORAIS, E.S.; SANTOS, M.L.; CREMON, E.H.; STEVAUX, J.C. Foodplain evolution in a confluence zone: Paraná and Ivaí rivers, Brasil. **Geomorphology**, 257, 1-9, DOI: 10.1016/j.geomorph.2015.12.017.
36. MOSLEY, M. P. An experimental study of channel confluences. **Journal of Geology**, v. 84, n. 5, p. 535-562, 1976.
37. MUELLER, D. S.; WAGNER, C. R.; REHMEL, M. S; OBERG, K. A.; RAINVILLE, F. **Measuring discharge with acoustic Doppler current profilers from a moving boat**. U.S. Geological Survey Techniques and Methods, book 3, chap. A22, 2013, p. 95.
38. NASCIMENTO, A. Z. A. **Características hidro-geomorfológicas do baixo curso dos rios Solimões e Negro, e sua confluência, Amazonas, Brasil**. Dissertação (Mestrado em Geografia) – Programa de Pós-graduação em Geogafia, Universidade Federal do Amazonas, Manaus. 2016. 63p.
39. ORFEO, O. **Sedimentologia del Rio Paraná en el área de confluência con el Rio Paraguay.** Tese (Doutorado) – Programa de Pós-graduação de la Facultad de Ciências Naturales y Museo, Universidad Nacional de La Plata, Corrientes, 1995. 289p.
40. PAES, R. J. **Análise da dinâmica do fluxo na confluência dos rios Paraná e Paranapanema.** Guarulhos, 2007. Dissertação (Mestrado em Análise Geoambiental) – Programa de Pós-graduação em Análise Geoambiental, Universidade de Guarulhos, Guarulhos, 2007. 53 p.
41. PARSONS, D. R.; BEST, J. L.; LANE, S. N.; ORFEO, O. HARDY, R. J.; KOSTASCHUK, R. Form roughness and the absence of secondary flow in a large confluence-diffluence, Rio Paraná, Argentina. **Earth Surface Processes and Landforms**, v. 32, p. 155-162, 2007.
42. PARSONS, D. R.; BEST, J. L.; LANE, S. N.; KOSTASCHUK, R. A.; HARDY, R. J.; ORFEO, O.; AMSLER, M. L.; SZUPIANY, R. N. Large River channel confluence. In: RICE, S.P.; ROY, A.G.; RHOADS, B.L. **River confluences, tributaries and the fluvial network.** John Wiley & Sons Ltd. v.1, 2008. Cap. 5, p. 73-91.
43. PARSONS, D. R.; JACKSON, P. R.; CZUBA, J. A.; ENGEL, F. L.; RHOADS, B. L.; ORBERG, K. A.; BEST, J. L; MUELLER, D. S.; JOHNSON, K. K.; RILEY, J. D. Velocity Mapping ToolBox (VMT): a processing and visualization suite for moving-vessel ADCP measurements. **Earth Surface Processes and Landforms**, v. 38, p. 1244-1260, 2013.
44. PLOTLY/PLOTLY.py is licensed under the MIT License.
45. RHOADS, B. L.; JOHNSON, K. K.; Three-dimensional flow structure, morphodynamics, suspended sediment, and thermal mixing at an asymmetrical river confluence of a straight tributary and curving main channel. **Geomorphology**, v. 323, p. 51-69, 2018.
46. RHOADS, B. L.; RILEY, J. D.; MAYER, D. R. Response of bed morphology and bed material texture to hydrological conditions at an asymmetrical stream confluence. **Geomorphology**, n. 109, p. 161-173, 2009.
47. ROY, A. G.; ROY, R.; BERGERON, N. Hydraulic geometry and changes in flow velocity at a river confluence with coarse bed material. **Earth Surface Processes and Landforms**, v. 13, n. 7, p. 583-598, 1988.
48. ROY, A. G. Introduction to Part I: river channel confluences. In: RICE, S.P.; ROY, A.G.; RHOADS, B.L. **River confluences, tributaries and the fluvial network**. John Wiley & Sons Ltd. v. 1, 2008. Cap. 2, p. 13-16.
49. RICE, S. P.; RHOADS, B. L.; ROY, A. G. Introduction: river confluences, tributaries and the fluvial network. In: RICE, S.P.; ROY, A. G.; RHOADS, B.L. **River confluence, tributaries and the fluvial network**. John Wiley & Sons Ltd,. 1, 2008. Cap. 1, p. 1-9.

50. ROSOVSKII, J. L. 1957. Flow of water in bends of open channels. In: **Academy of Sciences of the Ukrainian SSR**; Kiev [translated from Russian by the Israel Program for Scientific Translations, Jerusalem, 1961].
51. SANTOS, V. C.; STEVAUX, J. C. Processos fluviais e morfologia em confluência de canais: uma revisão. **Revista Brasileira de Geomorfologia**, v. 18, n. 01, p. 1-15, 2017.
52. SANTOS, V. C.; STEVAUX, J. C.; SZUPIANY, R. N. Confluence analysis at basin scale in a tropical bedrock river – The Ivaí River, Southern Brazil. **Journal of South American Earth Sciences**, v. 116, p. 1-13, 2022. DOI: 10.1016/j.jsames.2022.103877
53. SANTOS, L. J C.; OKA-FIORI, C.; CANALI, N. E.; FIORI, A. P.; SILVEIRA, C. T.; SILVA, J. M. F.; ROSS, J. L. S. Mapeamento geomorfológico do estado do Paraná. **Revista Brasileira de Geomorfologia,** v. 7, n. 2, p. 3-12, 2006.
54. SIQUEIRA, L. F.; FILIZOLA JUNIOR, N. P. Estudo hidrológico do efeito de barramento hidráulico no rio Tarumã-Açu, Manaus, AM. **Revista Brasileira de Geomorfologia**, v. 22, n. 1, p. 315-335, 2021.
55. STEVAUX, J. C; MARTINS, D. P; MEURER, M. Changes in a large regulated tropical river: The Paraná River downstream from the Porto Primavera Dam, Brazil. **Geomorphology**, v. 113, p. 230-238, 2009.
56. STEVAUX, J. C.; LATRUBESSE, E. M. **Geomorfologia fluvial**. Oficina de Textos. São Paulo, 2017.
57. STEVAUX, J. C.; GON, P. P.; LELI, I. T.; FUJITA, R. H. Why do large rivers tend to form multichannel? A field study in the Upper Paraná River. **Revista Brasileira de Geomorfologia**, v. 22, n. 4, p. 967-985, 2021. DOI:10.20502/rbg.v22i4.2014
58. SUGUIU, K. **Introdução à sedimentologia**. São Paulo: Ed. Edgard Blucher, 1973.
59. SUKHODOLOV, A. N.; RHOADS, B. L. Field investigation of three-dimensional flow structure at stream confluences: 2 Turbulence. **Water Resources Research**, v. 37, p. 2411-2424, 2001.
60. SZUPIANY, R. N.; AMSLER, M.L.; PARSONS, D. R.; BEST, J. L. Morphology, flow structure, and suspended bed sediment transport at two large braid-bar confluences. **Water Resources Research**, v. 45, p. 1-19, 2009.
61. SZUPIANY, R. N.; AMSLER, M. L.; HERNANDEZ, J.; PARSONS, D. R.; BEST, J. L.; FORNARI, E.; TRENTO, A. Flow fields, bed shear stresses, and suspended bed sediment dynamics in bifurcations of a large river. **Water Resources Research**, v. 48, p. 1-20, 2012.
62. WEBER, L. J., ASCE, M.; SCHUMATE, E. D.; MAWER, N. Experiments on flow at a 90º open-channel junction. Journal of Hydraulic Engineering, v. 127, p. 340-350, 2001.
63. WEIBEL, C. L.; SZUPIANY, R.; LATOSINSKI, F.; AMSLER, M.; REPASCH, M. Sources and temporal dynamics of suspended sediment transport along the Paraná River system. **Journal of South America Earth Science**, v. 1, p. 1-13, 2022. DOI: 10.1016/j.jsames.2022.103968